PERGAMON

Computers & Fluids 30 (2001) 581–590

computers & fluids

www.elsevier.com/locate/compfluid

Low-Reynolds-number effects derived from direct numerical simulations of turbulent pipe flow

C. Wagner [a], T.J. Hüttl [b,*], R. Friedrich [b]

[a] *DLR, Bunsenstrasse 10, 37073 Göttingen, Germany*

[b] *Lehrstuhl für Fluidmechanik, TU München, Boltzmannstrasse 15, 85748 Garching, Germany*

Accepted 10 November 2000

Abstract

Fully developed, statistically steady and non-swirling turbulent flow through straight pipes of circular cross-section is investigated by means of direct numerical simulation. A finite-volume scheme of second-order accuracy and a semi-implicit time integration scheme of the same order of accuracy are used to integrate the incompressible Navier–Stokes equations on staggered grids. Significant low-Reynolds-number effects are observed in the mean axial velocity, the components of the Reynolds stress tensor, the pressure and vorticity fluctuations, the turbulent kinetic energy budget and two-point velocity correlations. It is confirmed that turbulence data obtained in the near-wall region do not scale on wall variables. Within the range of Reynolds numbers investigated, the non-dimensional streak spacing increases slightly with Re_τ.

1. Numerical method and computational details

The dynamics of turbulence of an incompressible Newtonian fluid is completely described by the Navier–Stokes equations, which read in dimensionless form:

$$\nabla \cdot \vec{\mathbf{u}} = 0, \tag{1}$$

$$\frac{\partial \vec{\mathbf{u}}}{\partial t} + (\vec{\mathbf{u}} \cdot \nabla)\vec{\mathbf{u}} = -\nabla p + \frac{1}{Re_\tau}\nabla^2 \vec{\mathbf{u}}. \tag{2}$$

* Corresponding author. Address: Fichtenstrasse 1, D-82178 Puchheim, Germany. Tel.: +49-89-8902-0957; fax: +49-89-1489-95242.

E-mail address: thomas@huettl.de (T.J. Hüttl).

0045-7930/01/$ - see front matter
PII: S0045-7930(01)00007-X

The velocity vector $\vec{\mathbf{u}}$ is non-dimensionalized with the friction velocity u_τ, the pressure with ρu_τ^2. Length and time scales are R, the pipe radius, and R/u_τ. The turbulence Reynolds number is defined as $Re_\tau = Ru_\tau/\nu$. It can be interpreted as the ratio of an outer length scale R and an inner length scale ν/u_τ. Eqs. (1) and (2) are integrated in a cylindrical (z, φ, r) coordinate system, using Schumann's [4] finite volume technique without subgrid scale model, which essentially leads to second-order accurate central flux differences in space. The instantaneous pressure gradient is split into a mean value $-\nabla P$ which balances the viscous friction at the wall and equals 2 when scaled with R and u_τ. The pressure fluctuations p' and the instantaneous velocity vector $\vec{\mathbf{u}}$ are assumed periodic in axial direction, which makes sense when the pipe is at least $10R$ long. Staggered grids are used to integrate the spatially discrete momentum equation in time. The time-advancement scheme is second-order accurate and semi-implicit, i.e. all convection and diffusion terms containing derivatives in φ-direction are treated implicitly. The time step deduced from a linear stability analysis of the discrete equations takes convective and diffusive time scales into account. A fractional step method leads to a Poisson equation for the pressure which is solved directly, using FFT in axial and circumferential directions and a tridiagonal matrix algorithm. At the wall impermeability and no slip boundary conditions are satisfied.

The numerical method described is mass and energy conserving but has dispersive errors in the high wave numbers. It has, however, been confirmed by Choi et al. [3] that second-order accurate central schemes provide a spectral resolution of the velocity fluctuations for the same number of grid points.

The computational domain is a pipe of length $L = 10R$ and radius R. This domain is resolved by grid points which are equidistant in axial and circumferential directions, but non-equidistant in the radial direction. In terms of wall units, ν/u_τ, the grid spacing varies with the Reynolds number Re_τ, according to Table 1.

For all Reynolds numbers the grids have $(486 \times 240 \times 70)$ points. Based on bulk velocity and pipe diameter D the Reynolds numbers Re_D range from 5300 to 10 300. The simulations are started from uncorrelated initial data. After a certain transient time (roughly 24 convective time scales R/u_τ) in which correlations build up, a statistically steady state is reached which is independent of the initial conditions. This is the moment where time averaging of the data starts. The simulations were then run over more than 100 convective time scales, so that more than 200 statistically independent time levels could be used for averaging besides spatial averaging in z- and φ-directions. The smallest time step was 5×10^{-4} and about 250 h CPU time on a CRAY T94 were needed per case.

Table 1
Grid spacing in wall units for different Reynolds numbers

Reynolds number, Re_τ	Δz^+	$(r\,\Delta\varphi^+)_{\max}$	$\Delta r^+_{\min}$	$\Delta r^+_{\max}$
180	3.7	4.70	0.36	4.32
250	5.13	6.53	0.5	6.0
320	6.58	8.36	0.64	7.68

2. Results

In fully developed pipe flow the balance of mean axial momentum reads in wall units:

$$\frac{\mathrm{d}\langle u_z^+\rangle}{\mathrm{d}y^+} + \langle u_z^{+\prime} u_r^{+\prime}\rangle = 1 - y^+/R^+, \tag{3}$$

where $\langle u_z^+\rangle = \langle u_z\rangle/u_\tau$ and $y^+ = yu_\tau/\nu = R^+ - r^+$ is the dimensionless distance from the wall. R^+ equals the Reynolds number Re_τ. For infinitely large Reynolds number ($Re_\tau \to \infty$) this equation becomes

$$\frac{\mathrm{d}\langle u_z^+\rangle}{\mathrm{d}y^+} + \langle u_z^{+\prime} u_r^{+\prime}\rangle = 1 \tag{4}$$

and allows to compute the dimensionless turbulent kinetic energy production rate:

$$P_\infty^+ = \langle u_z^{+\prime} u_r^{+\prime}\rangle \frac{\mathrm{d}\langle u_z^+\rangle}{\mathrm{d}y^+} = \frac{\mathrm{d}\langle u_z^+\rangle}{\mathrm{d}y^+}\left(1 - \frac{\mathrm{d}\langle u_z^+\rangle}{\mathrm{d}y^+}\right), \tag{5}$$

the maximum of which is $(P_\infty^+)_{\max} = 0.25$. This is the upper bound of the TKE production peak. It helps to check the quality of the computation. Fig. 1 contains mean velocity profiles for the three Reynolds numbers in Table 1. For $Re_\tau = 180$ a comparison with LDA measurements of Westerweel et al. [5] is provided. It shows good agreement. The universal law contained in the figure is that derived by Zagarola [6] from measurements in a Re_D number range between 3×10^4 and 4×10^6. We conclude from this figure that even at $Re_D = 10\,300$ a logarithmic overlap region has not yet developed. In that respect pipe flow differs from channel flow (with large or infinite aspect ratio) where a log region appears much earlier. Profiles of the mean velocity normalized with the centerline velocity as a function of r/R reveal only minor Reynolds number effects in the core

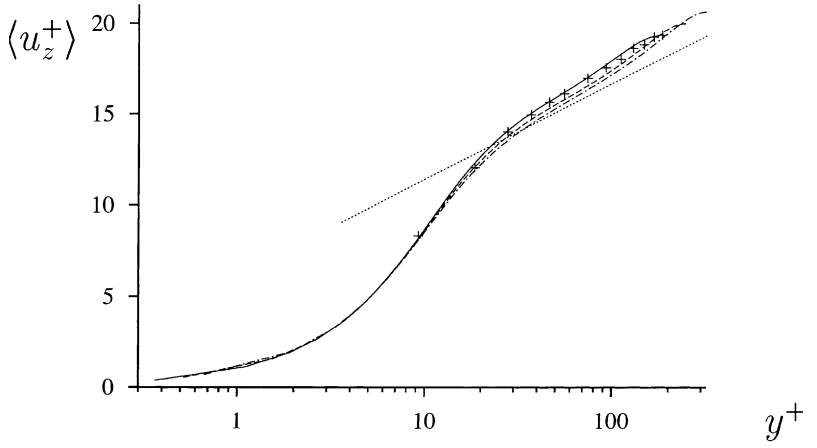

Fig. 1. Mean axial velocity $\langle u_z^+\rangle$ over wall distance y^+: (—) $Re_\tau = 180$, (- - -) $Re_\tau = 250$, (· · · · ·) $Re_\tau = 320$, (· · ·) $\left[u_z^+ = (\ln(y^+)/0.436) + 6.13\right]$, (+) LDA [5].

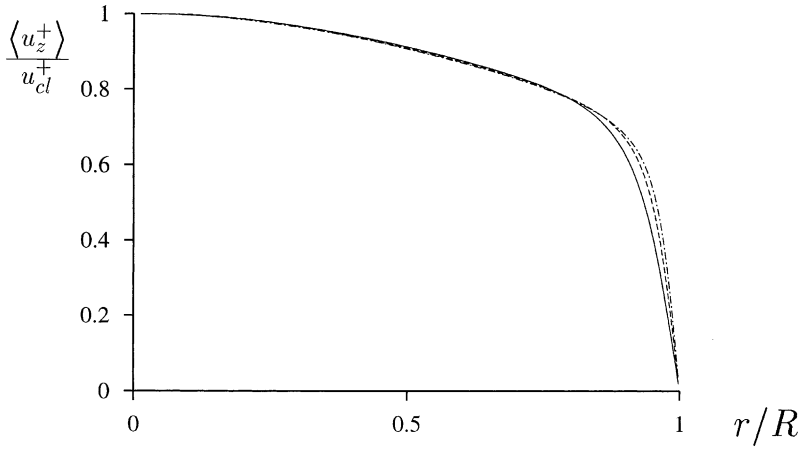

Fig. 2. Mean axial velocity $\langle u_z \rangle / u_\tau$ over pipe radius r/R: (—) $Re_\tau = 180$, (- - -) $Re_\tau = 250$, (· - - - ·) $Re_\tau = 320$.

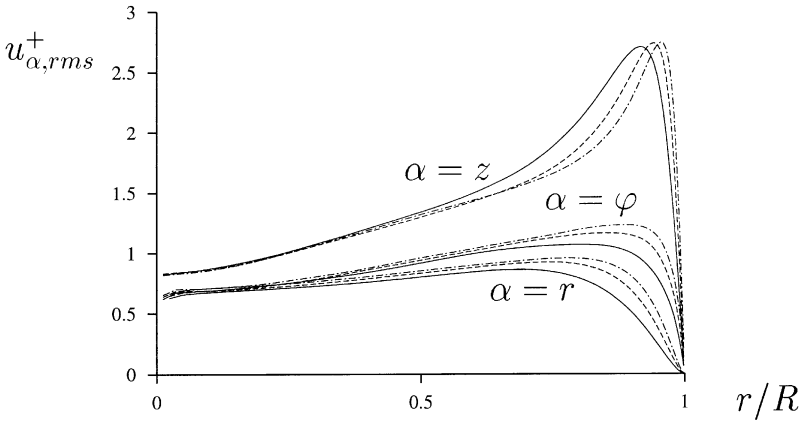

Fig. 3. Rms values over pipe radius r/R: (—) $Re_\tau = 180$, (- - -) $Re_\tau = 250$, (· - - - ·) $Re_\tau = 320$.

region, but steeper near-wall velocity gradients (see Fig. 2). Similar effects are also observed in the rms velocity fluctuations in Fig. 3. When plotted as functions of the pipe radius, the locations of their maxima approach the wall as Re_τ increases. When $u^+_{z,\mathrm{rms}}$ is plotted against y^+ (not shown) the location of its maximum is essentially unchanged. This is in agreement with the situation in a plane channel [2]. While the maximum value of $u^+_{z,\mathrm{rms}}$ shows only a negligible increase with Re_τ, the maxima of $u^+_{\varphi,\mathrm{rms}}$ and $u^+_{r,\mathrm{rms}}$ increase remarkably. From Taylor series expansions of the velocity fluctuations about their wall values (see e.g. Ref. [1]) it is expected that $u^+_{z,\mathrm{rms}}$ and $u^+_{\varphi,\mathrm{rms}}$ divided by y^+ should tend asymptotically to constant values near the wall. On the other hand, it is $u^+_{r,\mathrm{rms}}/y^{+2}$ that should become constant asymptotically. The logarithmic scale for y^+ highlights this behavior for the turbulence intensities in Figs. 4–6 and for the Reynolds shear stress in Fig.7. Obviously, a scaling with the standard wall variables u_τ and ν/u_τ is not appropriate to collapse the curves for

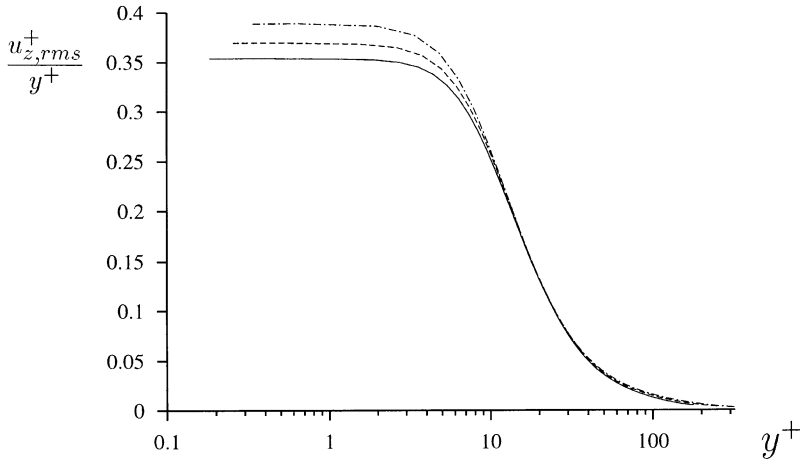

Fig. 4. Rms value: (—) $Re_\tau = 180$, (- - -) $Re_\tau = 250$, (· - · - ·) $Re_\tau = 320$.

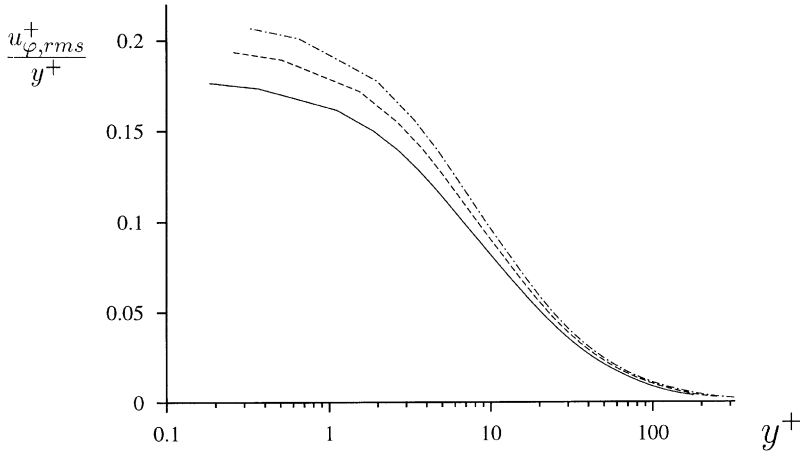

Fig. 5. Rms value: (—) $Re_\tau = 180$, (- - -) $Re_\tau = 250$, (· - · - ·) $Re_\tau = 320$.

different Reynolds numbers. As Antonia and Kim [1] point out, a scaling with the Kolmogorov length and velocity scales

$$\eta_w = (\nu^3/\epsilon_w)^{1/4}, \qquad v_w = (\nu\epsilon_w)^{1/4} \tag{6}$$

(ϵ_w being the TKE dissipation rate at the wall) collapses the profiles in the wall region up to the maximum value of the corresponding variable much better. This is demonstrated in Fig. 8 for the axial rms velocity fluctuation, where both scalings are contrasted. Variables with a star are non-dimensionalized with η_w and v_w viz:

$$u^*_{z,\mathrm{rms}} = u_{z,\mathrm{rms}}/v_w, \qquad y^* = y/\eta_w. \tag{7}$$

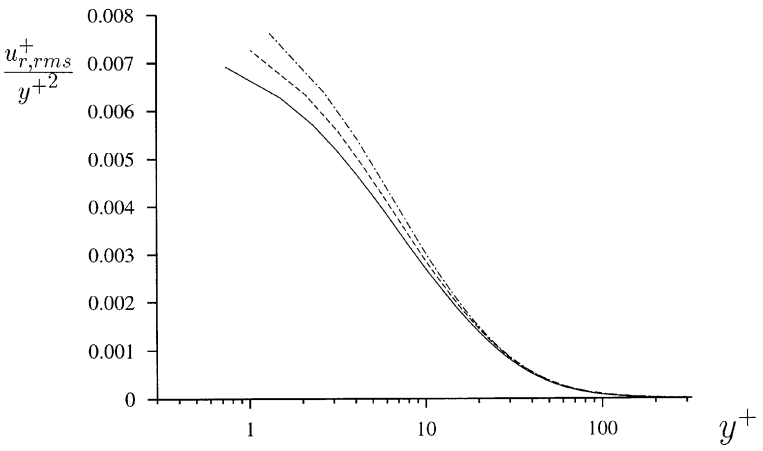

Fig. 6. Rms value: (—) $Re_\tau = 180$, (- - -) $Re_\tau = 250$, (· - - - ·) $Re_\tau = 320$.

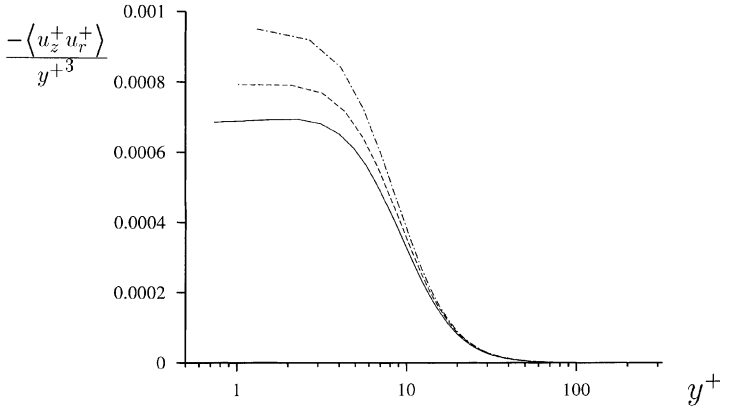

Fig. 7. Reynolds shear stress $\langle u_z^+ u_r^+ \rangle$: (—) $Re_\tau = 180$, (- - -) $Re_\tau = 250$, (· - - - ·) $Re_\tau = 320$.

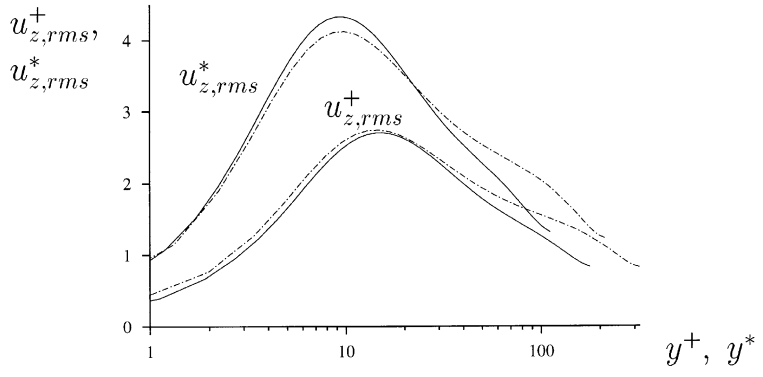

Fig. 8. Rms value, $u^+_{z,\mathrm{rms}}$ is normalized with u_τ and drawn over y^+; $u^*_{z,\mathrm{rms}}$ is normalized with $v_\mathrm{w} = (\nu\epsilon_\mathrm{w})^{1/4}$ and drawn over $y^* = y/\eta_\mathrm{w}$: (—) $Re_\tau = 180$, (· - - - ·) $Re_\tau = 320$.

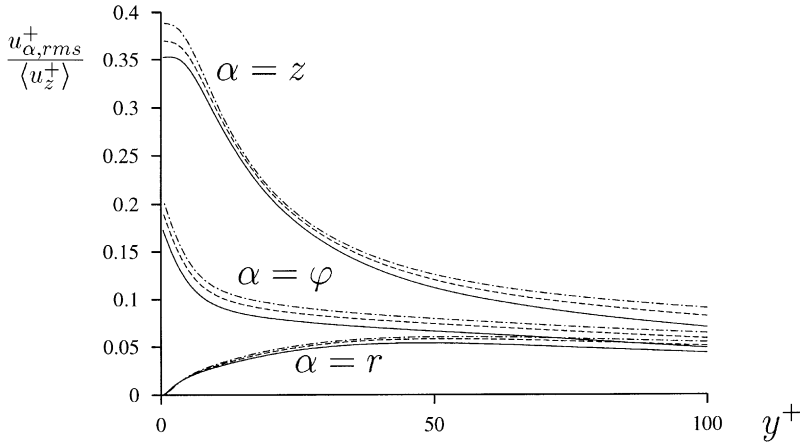

Fig. 9. Rms value: (—) $Re_\tau = 180$, (- - -) $Re_\tau = 250$, (· - · - ·) $Re_\tau = 320$.

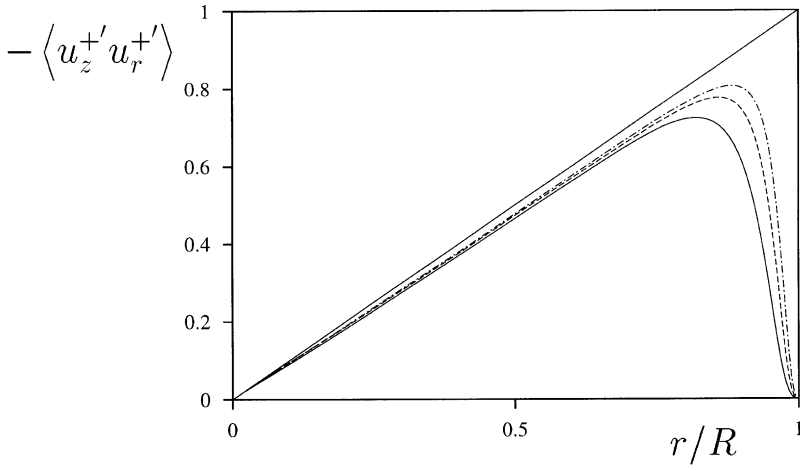

Fig. 10. Reynolds shear stress $\langle u_z^{+\prime} u_r^{+\prime} \rangle$: (—) $Re_\tau = 180$, (- - -) $Re_\tau = 250$, (· - · - ·) $Re_\tau = 320$.

A scaling of $u_{\alpha,\mathrm{rms}}$ with $\langle u_z(r) \rangle$ in Fig. 9 shows that the axial and circumferential components have again asymptotic wall values and that their amplitudes increase with the Reynolds number. The dimensionless Reynolds shear stress versus r/R is plotted in Fig. 10. The limiting curve for infinite Reynolds number, $Re_\tau \to \infty$ appears as the straight solid line. For finite Re_τ this line represents the sum of the viscous and Reynolds shear stress. Rms pressure fluctuations are shown in Figs. 11 and 12. The Reynolds number effect becomes negligible in the wall region, when p_{rms} is scaled with the turbulent kinetic energy k. The rms vorticity fluctuations are amplified with increasing Reynolds number. This is especially true for the streamwise component, $\omega_{z,\mathrm{rms}}$, see Fig. 13 and indicates a strengthening of the quasi-streamwise vortices. The intensification of the wall values of the φ- and

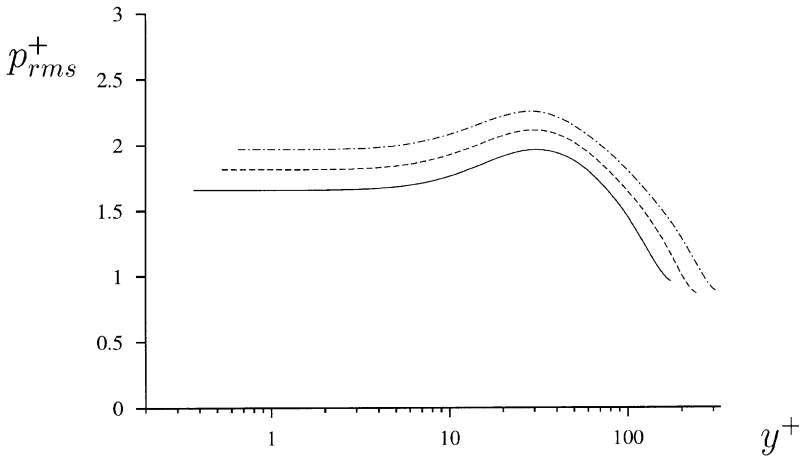

Fig. 11. Rms value of the pressure: (—) $Re_\tau = 180$, (- - -) $Re_\tau = 250$, (· - · - ·) $Re_\tau = 320$.

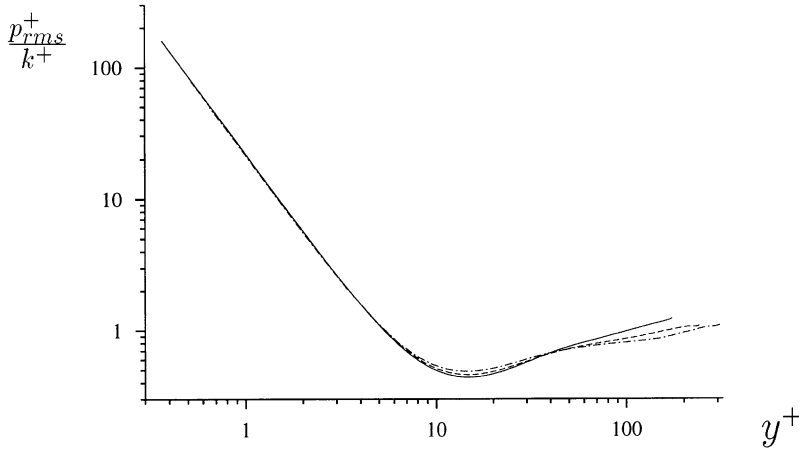

Fig. 12. Rms value of the pressure normalized with the turbulent kinetic energy k: (—) $Re_\tau = 180$, (- - -) $Re_\tau = 250$, (· - · - ·) $Re_\tau = 320$.

z-components is consistent with the increased TKE dissipation rate (DS) at the wall, see Fig. 14. This entails corresponding effects in the viscous diffusion term (VD) at the wall. The production term (PR) approaches its maximum value of 0.25 at $y^+ \approx 14$ as $Re_\tau \to \infty$. Fig. 15, finally, contains two-point correlations in φ-direction of the axial velocity fluctuations for the three Reynolds numbers $Re_\tau = 180$, 250 and 320. The minima of the axial velocity correlations provide half the streak spacing. A slight increase in the streak spacing λ^+ from, approximately, 114 to 128 can be observed, when Re_τ increases from 180 to 320.

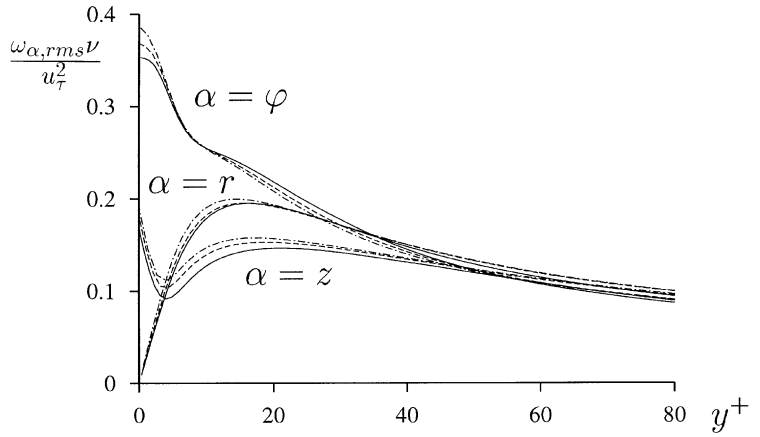

Fig. 13. Rms value of vorticity: (—) $Re_\tau = 180$, (- - -) $Re_\tau = 250$, (· - - - ·) $Re_\tau = 320$.

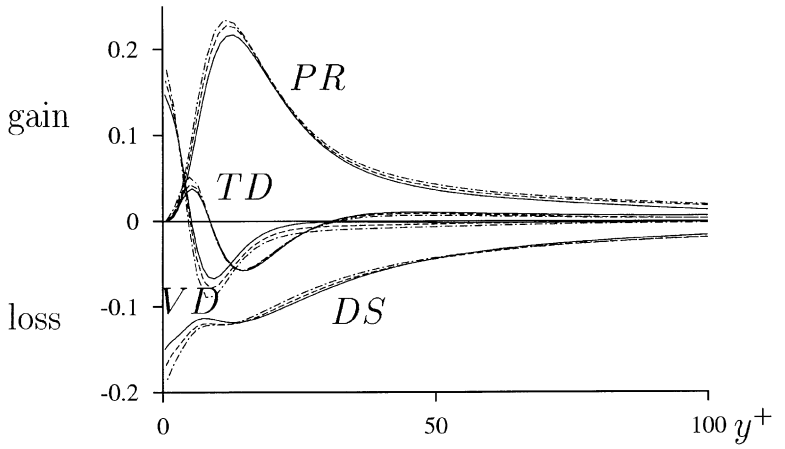

Fig. 14. Budget of the turbulent kinetic energy. The symbols PR, DS, TD and VD stand for production and dissipation rates, turbulent and viscous diffusion. All terms are non-dimensionalized by u_τ^4/ν: (—) $Re_\tau = 180$, (- - -) $Re_\tau = 250$, (· - - - ·) $Re_\tau = 320$.

3. Conclusions

Direct numerical simulations of turbulent pipe flow have been performed for three different Reynolds numbers and the effects of Reynolds number on turbulence quantities are investigated. In contrast to plane channel flow, a logarithmic overlap region does not exist for Reynolds numbers up to $Re_D = 10\,300$. Nevertheless, the effects of increasing Reynolds number are qualitatively the same as for turbulent plane channel flow: the locations of the maxima of the rms velocity fluctuations and of the Reynolds shear stress $\langle u_s'' u_r'' \rangle$ approach the wall as Re_τ increases.

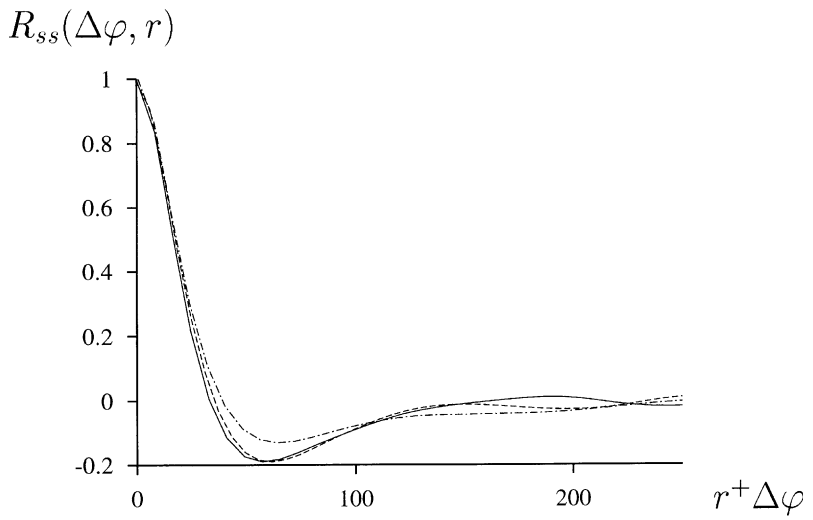

Fig. 15. Correlations function in φ-direction, taken at $y^+ = 14$: (—) $Re_\tau = 180$, (- - -) $Re_\tau = 250$, (· - · - ·) $Re_\tau = 320$.

The terms $u^+_{s,\mathrm{rms}}/y^+$, $u^+_{\varphi,\mathrm{rms}}/y^+$, $u^+_{r,\mathrm{rms}}/y^{+^2}$ and $\langle u''_s u''_r\rangle/y^{+^3}$ tend asymptotically to constant values near the wall. These asymptotic values depend on the Reynolds number. It has been shown that scaling with the Kolmogorov length and velocity scales is more approximate than scaling with standard wall variables.

References

[1] Antonia RA, Kim J. Low-Reynolds-number effects on near-wall turbulence. J Fluid Mech 1994;276:61–80.
[2] Antonia RA, Teitel M, Kim J, Growne LWB. Low-Reynolds number effects in fully developed turbulent channel flow. J Fluid Mech 1992;236:579–605.
[3] Choi H, Moin P, Kim J. Turbulent drag reduction: studies of feedback control and flow over riblets. Thermoscience Division, Department of Mechanical Engineering, Stanford, Report no. TF-55, 1992.
[4] Schumann U. Subgrid scale model for finite difference simulations of turbulent flows in plane channels and annuli. J Comput Phys 1995;18:376–404.
[5] Westerweel J, Adrian RJ, Eggels JGM, Nieuwstadt FTM. Measurements with particle image velocimetry on fully developed turbulent pipe flow at low-Reynolds number. Proceedings of the 6th International Symposium on Applications of Laser Technique to Fluid Mechanics, Lisbon, Portugal, 20–23 July, 1992.
[6] Zagarola MV. Mean-flow scaling of turbulent pipe flow. PhD Thesis, USA: Princeton University; 1996.